Title: Renormalization - 2

Date: Jul 23, 2013 04:40 PM

URL: http://pirsa.org/13070055

Abstract:

Coarse Graining Methods for Spin Net and Spin Foam Models

Mercedes Martín-Benito

Perimeter Institute for Theoretical Physics

[Dittrich, Eckert, MMB, 1109.4927, New J. Phys. '12]
[Dittrich, MMB, Schnetter, 1306.2987]
[Dittrich, MMB, Steinhaus, to appear]

PERIMETER INSTITUTE FOR THEORETICAL PHYSICS

LOOPS '13

July 23, 2013

Introduction

- Spin Foam models : non-perturbative candidates for quantum gravity
  [Barret, Crane, Rovelli, Reisenberger, Livine, Speziale, Engle, Pereira, Freidel, Krasnov,...]
- Microscopic description of space-time
- Regularization of the path integral based on a discretization of space-time:
  ⟶ lattice (two-complex)
- No (background) lattice constant: Generalized lattice gauge theories
- Lattice regularization in general breaks diffeomorphism symmetry

- Q: Large scale physics of spin foams?
  Limit with many building blocks and small discretization scale?
  - Do they flow under renormalization to a continuum space-time?
- The complexity of the models has prevented an explicit study
- First step to answer this question :
  ⟶ to analyze simplified models which capture essential features of SF's

Introduction

- Simplifications :

  - Lie groups ⟶ finite groups: baby spin foams [Bahr, Dittrich, Ryan, 1103.6264]
  - General two-complex ⟶ regular lattice
  - Dimensionally reduced models (one-complex) ⟶ spin net models

- Spin Net models : retain key ingredient of SF's

  ⟶ Simplicity Constraints

- It is doable to analyze their renormalization flow by using coarse graining techniques from condense matter and statistical physics

- Tensor network renormalization

  ⟶ Behavior under coarse graining

  ⟶ Restoration of symmetries in the continuum limit

Outline

1. Spin Foams basics
2. Spin Nets
3. Tensor network renormalization group approach
4. Spin nets based on S_3
5. Outlook
6. Conclusions

Spin foams basics

- **Generalization of lattice gauge theories**

i. **Standard lattice gauge theory**

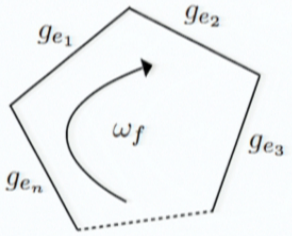

$g_i \in G$

face weight : $\omega_f(g) = \omega_f(g' g g'^{-1})$

$$Z \sim \sum_{g_e} \prod_f \omega_f(g_{e_1} \cdots g_{e_n})$$

face holonomy

group elements attached to edges

In dual variables (group Fourier transform)

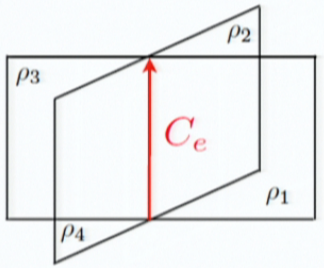

$$Z \sim \sum_{\rho_f} \left(\prod_f \tilde{\omega}_f(\rho_f) \right) \prod_e P_e(\{\rho_f\}_f \supset e)$$

Haar Projector (intertwiner)

projects on the inv. subspace of $\otimes_{f \supset e} (V_{\rho_f} \otimes V^*_{\rho_f})$

Spin foams basics

ii. Spin Foams in Spin representation

- Background independence : $\tilde{\omega}_f = 1$
- Replaces Haar projector by a projector in a smaller subspace

$$Z \sim \sum_{\rho_f} \prod_e C_e(\{\rho_f\}_{f \supset e})$$

simplicity constraints

$$P_e(\{\rho_f\}_{f\supset e}) \left[\prod_{f \supset e} \tilde{E}_f(\rho_f) \right] P_e(\{\rho_f\}_{f\supset e})$$

different from Haar projector in general

Fixed points and phases :

- Those of lattice gauge theory :
  - BF = weak coupling limit : C_e is the Haar projector
  - degenerate = strong coupling limit : all ρ_f frozen to the trivial rep.
- Any additional fixed point ?

5

Spin Nets

- **1-dimensional reduction of SF's :**

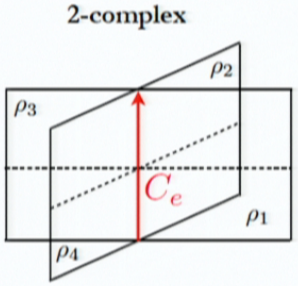

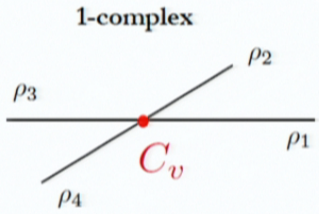

$$Z \sim \sum_{\rho_f} \prod_{e} C_e(\{\rho_f\}_{f \supset e}) \longrightarrow Z \sim \sum_{\rho_e} \prod_{v} C_v(\{\rho_e\}_{e \supset v})$$

local gauge symmetry → global symmetry

Similarity between lattice gauge theories in 4D and corresponding "edge" models in 2D.

[Kogut, Rev. Mod. Phys. 51 (1979)]

Spin Nets as vertex models

$$Z \sim \sum_{\rho_e} \prod_v C_v(\{\rho_e\}_{e\supset v})$$

$$\mathcal{H}_e = \oplus_{\rho_e}(V_{\rho_e} \otimes V_{\rho_e^*})$$

$$C_v(\{\rho_e\}_{e\supset v}) = P(\{\rho_e\}_{e\supset v})\Big[\prod_{e\supset v} \tilde{E}_e(\rho_e)\Big]P(\{\rho_e\}_{e\supset v})$$

Haar projector

weights for intertwiners (determine dynamics of models)

- **Regular square lattice**

$$Z \sim \mathrm{tTr}\left(\quad\right)$$

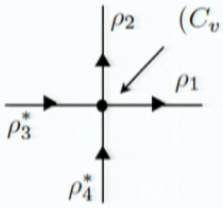

$(C_v)_{1234} \in \otimes_{e=1}^4 \mathcal{H}_e$,

$\rho_e,\ m_e,\ m_e'$

$|\rho_e, m_e, m_e'\rangle$

In this basis : $(C_v)_{m_1 m_1' m_2 m_2' m_3 m_3' m_4 m_4'}(\rho_1, \rho_2, \rho_3^*, \rho_4^*)$

Global gauge invariance $\longrightarrow$ $\rho_1 \otimes \rho_2 \supset \rho_T \subset \rho_3 \otimes \rho_4$

In the recoupling basis the tensor diagonalizes per blocks

Spin Nets as vertex models

$$Z \sim \sum_{\rho_e} \prod_v C_v(\{\rho_e\}_{e\supset v})$$

$$\mathcal{H}_e = \oplus_{\rho_e}(V_{\rho_e} \otimes V_{\rho_e^*})$$

$$C_v(\{\rho_e\}_{e\supset v}) = P(\{\rho_e\}_{e\supset v})\Big[\prod_{e\supset v} \tilde{E}_e(\rho_e)\Big]P(\{\rho_e\}_{e\supset v})$$

Haar projector

weights for intertwiners (determine dynamics of models)

- **Regular square lattice**

$$Z \sim \mathrm{tTr}\left(\right.$$ 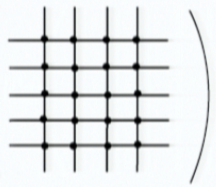 $$\left.\right)$$

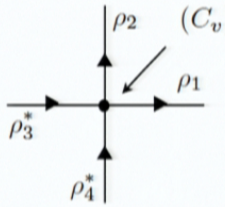

$\rho_e,\ m_e,\ m'_e$

$|\rho_e, m_e, m'_e\rangle$

In this basis : $(C_v)_{m_1 m'_1 m_2 m'_2 m_3 m'_3 m_4 m'_4}(\rho_1, \rho_2, \rho_3^*, \rho_4^*)$

Global gauge invariance $\longrightarrow$ $\rho_1 \otimes \rho_2 \supset \rho_T \subset \rho_3 \otimes \rho_4$

In the recoupling basis the tensor diagonalizes per blocks

Spin Nets in recoupling basis

To recoupling basis : $|\rho_T, \rho'_T, m_T, m'_T\rangle = \sum_{m_1,m_2,m'_1,m'_2}$ 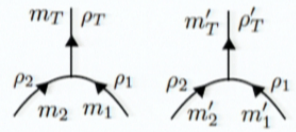 $|\rho_1, m_1, m'_1\rangle \otimes |\rho_2, m_2, m'_2\rangle$

Clebsch - Gordan coefficients

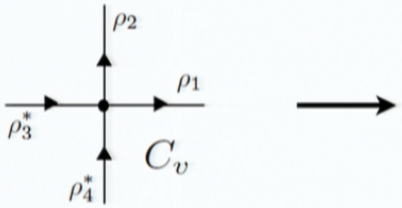

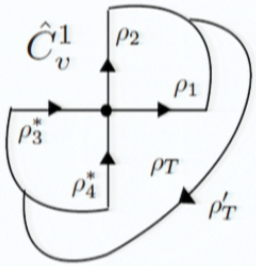

$\hat{C}^1_v(\rho_1, \rho_2, \rho^*_3, \rho^*_4, \rho_T, \rho'_T)$

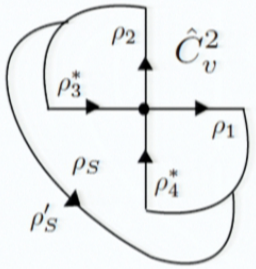

$\hat{C}^2_v(\rho_1, \rho_2, \rho^*_3, \rho^*_4, \rho_S, \rho'_S)$

Global gauge invariance ⟶ **blocks labelled by** (ρ_T, ρ'_T) **independent on** (m_T, m'_T)

Intertwiner chanel

Relation between $\hat{C}_v^2$ and $\hat{C}_v^1$

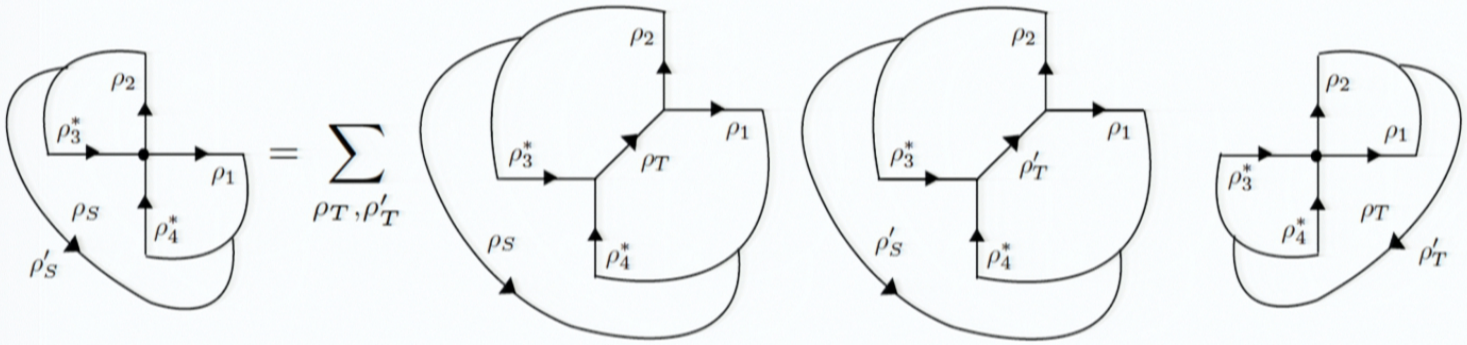

$$\hat{C}_v^2 = \sum_{\rho_T,\rho_T'} \begin{Bmatrix} \rho_S & \rho_4 & \rho_1 \\ \rho_T & \rho_2 & \rho_3 \end{Bmatrix} \begin{Bmatrix} \rho_S' & \rho_4 & \rho_1 \\ \rho_T' & \rho_2 & \rho_3 \end{Bmatrix} \hat{C}_v^1$$

6j - recoupling symbol

Coarse graining via tensor network methods

- Blocking procedure

  - Can deal with complex amplitudes
  - Direct access to structure of fixed points

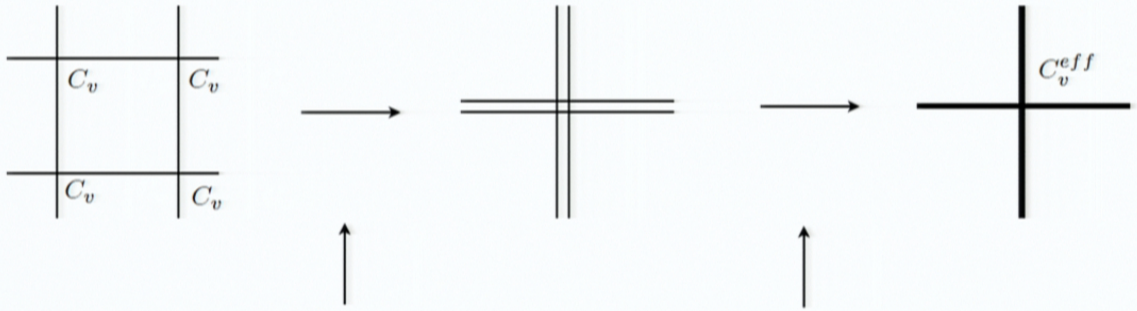

Embedding map : coarser $\longleftrightarrow$ finer

$m, m' = 1, \cdots, d$

$m'' = 1, \cdots, \chi < d^2$

bond dimension

- To retain relevant d.o.f $\longrightarrow$ singular value decomposition

Tensor Renormalization Group

[Levin &Nave, Gu&Wen, Vidal, ... 00's+]

1. **Regard 4-valent tensors as matrices : diagonal per blocks**

$$\hat{C}_v^1(\rho_1,\rho_2,\rho_3^*,\rho_4^*,\rho_T,\rho_T') = (M_1^{\rho_T,\rho_T'})_{A\ B}$$

$\{\rho_1,\rho_2\}$ $\{\rho_3^*,\rho_4^*\}$

$$\hat{C}_v^2(\rho_1,\rho_2,\rho_3^*,\rho_4^*,\rho_S,\rho_S') = (M_2^{\rho_S,\rho_S'})_{A\ B}$$

$\{\rho_2,\rho_3^*\}$ $\{\rho_4^*,\rho_1\}$

2. **Singular value decomposition for each block : symmetry preserving algorithm**

$$(M_1)_{A,B} = \sum_{m=1}^{\chi} (S_1)_{A,m}(S_2)_{B,m} \qquad (M_2)_{A,B} = \sum_{m=1}^{\chi} (S_3)_{A,m}(S_4)_{B,m}$$

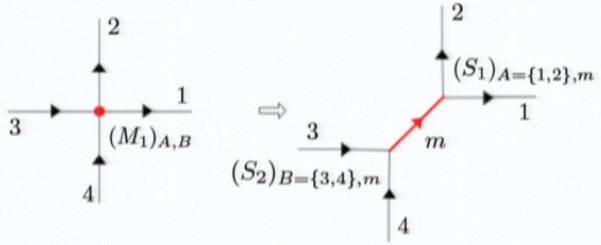

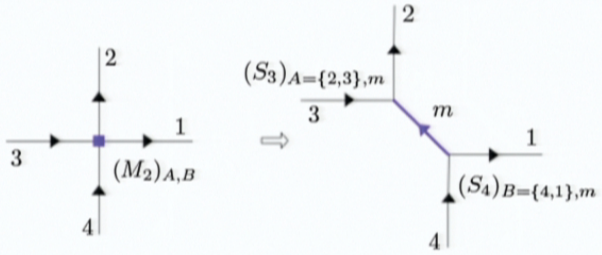

Tensor Renormalization Group

3. **Lattice splitting in 3-valent tensors**

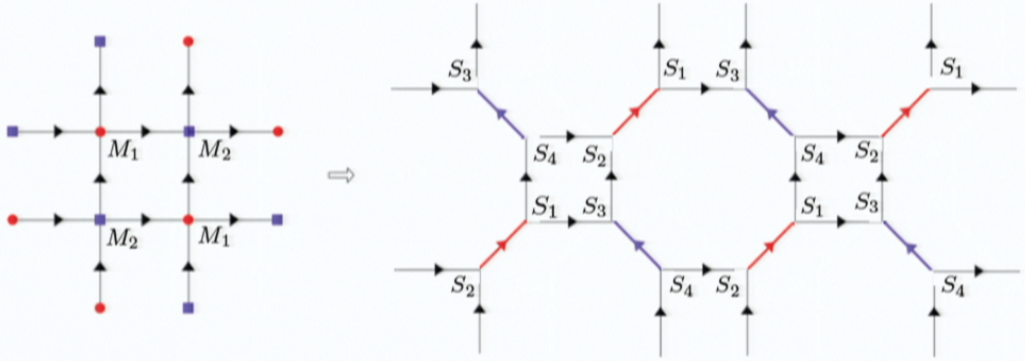

4. **Contraction to get effective tensor (rotated lattice)**

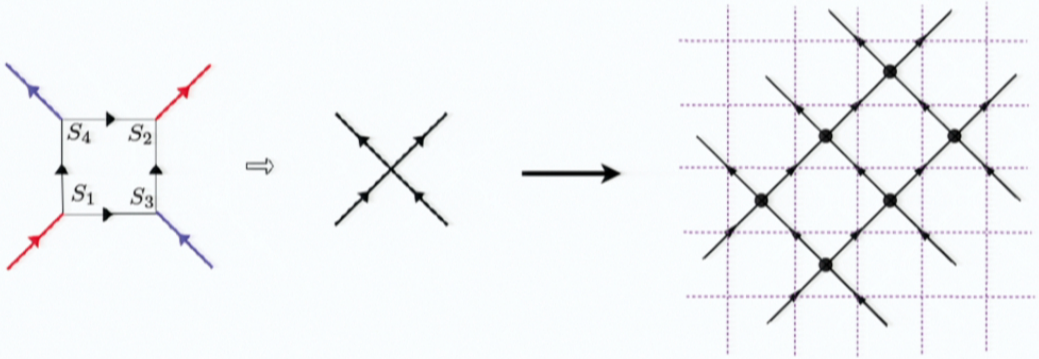

Flow equation

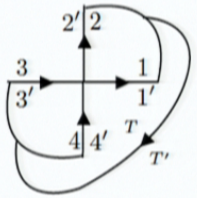

$$= \sum_{a,b,c,d}$$

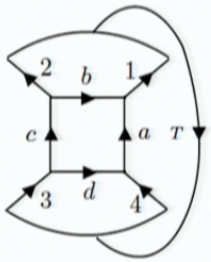

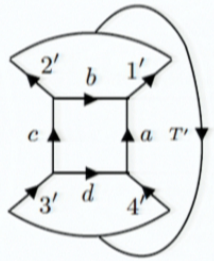

$\times\ S_2(b,a;m_1)$
$\times\ S_4(c,b;m_2)$
$\times\ S_1(d,c;m_3)$
$\times\ S_3(a,d;m_4)$

$(\hat{C}_v^1)^{eff}_{\rho_T,\rho_{T'}}(\rho_1,\rho_1',m1,\cdots,\rho_4^*,\rho_4'^*,m_4)$

$\uparrow$

$1,\cdots,\chi_1(\rho_1,\rho_1')$

$\|$

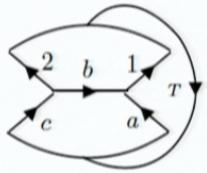

$$\sim \left\{ \begin{matrix} \rho_T & \rho_c & \rho_a \\ \rho_b & \rho_1 & \rho_2 \end{matrix} \right\}$$

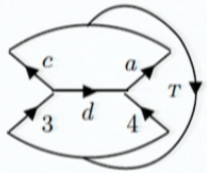

$$\sim \left\{ \begin{matrix} \rho_T & \rho_3 & \rho_4 \\ \rho_d & \rho_a & \rho_c \end{matrix} \right\}$$

Hilbert space on each edge: $\mathcal{H}_e = \oplus_{\rho_e,\rho_{e'}} \chi_e(\rho_e,\rho_{e'})(V_{\rho_e} \otimes V_{(\rho_e')^*})$

$\longrightarrow$ **under coarse graining we obtain an enlarged space of models**

Flow equation

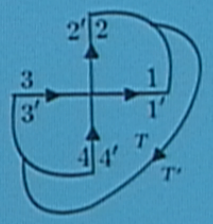

$$= \sum_{a,b,c,d}$$

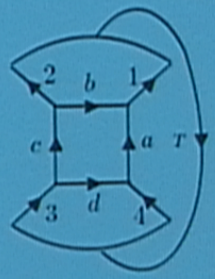

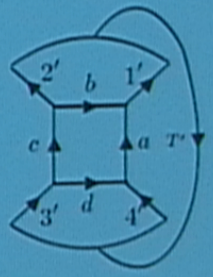

$\times\ S_2(b,a;m_1)$
$\times\ S_4(c,b;m_2)$
$\times\ S_1(d,c;m_3)$
$\times\ S_3(a,d;m_4)$

$$(\hat{C}^{-1}_v)^{efff}_{\rho_T,\rho_{T'}}(\rho_1,\rho_1',m1,\cdots,\rho_4^*,\rho_4'^*,m_4)$$

$$\uparrow$$

$$1,\cdots,\chi_1(\rho_1,\rho_1')$$

$$\|$$

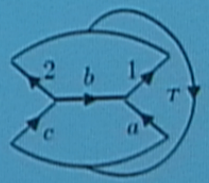

$$\sim \left\{ \begin{matrix} \rho_T & \rho_c & \rho_a \\ \rho_b & \rho_1 & \rho_2 \end{matrix} \right\}$$

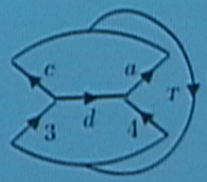

$$\sim \left\{ \begin{matrix} \rho_T & \rho_3 & \rho_4 \\ \rho_d & \rho_a & \rho_c \end{matrix} \right\}$$

Hilbert space on each edge: $\mathcal{H}_e = \oplus_{\rho_e,\rho_{e'}} \chi_e(\rho_e,\rho_{e'})(V_{\rho_e} \otimes V_{(\rho_e')^*})$

⟶ **under coarse graining we obtain an enlarged space of models**

Intertwiner dynamics

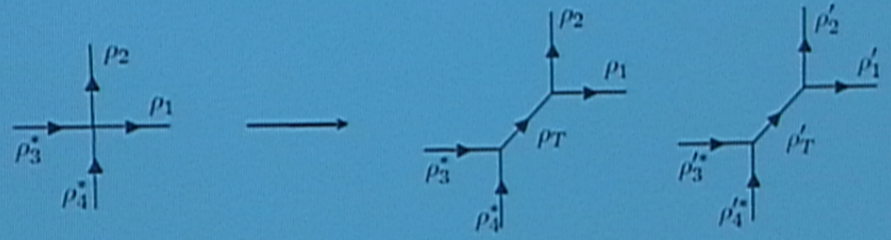

(ρ_T, ρ_T') Intertwiner chanel

$\mathcal{H}_e = \oplus_{\rho_e}(V_{\rho_e} \otimes V_{\rho_e^*})$

$\mathcal{H}_e = \oplus_{\rho_e,\rho_{e'}} \chi_e(\rho_e, \rho_{e'})(V_{\rho_e} \otimes V_{(\rho_e')^*})$

- Standard lattice gauge theory : $\rho' = \rho^*$
- Simplicity constraints : $\rho' \neq \rho^*$, some representations are forbidden
- Factorizing models : ρ and ρ' decoupled

- we can consider just one copy: anyon models (in condensed matter)

$\mathcal{H}_e = \oplus_{\rho_e} V_{\rho_e}$

Particles coupled to Chern Simons
Continuum limit : critical phase (massless excitations)
Hamiltonian topologically protected against perturbations

Intertwiner dynamics

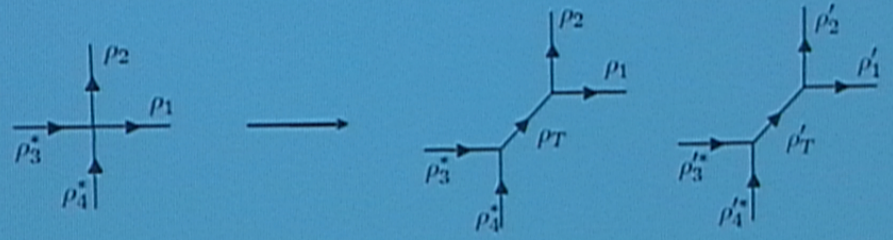

(ρ_T, ρ_T') Intertwiner chanel

$\mathcal{H}_e = \oplus_{\rho_e}(V_{\rho_e} \otimes V_{\rho_e^*})$

$\mathcal{H}_e = \oplus_{\rho_e,\rho_{e'}} \chi_e(\rho_e, \rho_{e'})(V_{\rho_e} \otimes V_{(\rho_e')^*})$

- Standard lattice gauge theory : $\rho' = \rho^*$
- Simplicity constraints : $\rho' \neq \rho^*$, some representations are forbidden
- Factorizing models : ρ and ρ' decoupled

  - we can consider just one copy: anyon models (in condensed matter)

$\mathcal{H}_e = \oplus_{\rho_e} V_{\rho_e}$

Particles coupled to Chern Simons
Continuum limit : critical phase (massless excitations)
Hamiltonian topologically protected against perturbations

Intertwiner dynamics

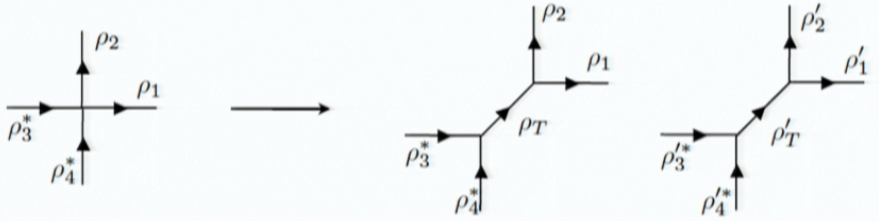

(ρ_T, ρ_T') Intertwiner chanel

$\mathcal{H}_e = \oplus_{\rho_e}(V_{\rho_e} \otimes V_{\rho_e^*})$

$\mathcal{H}_e = \oplus_{\rho_e,\rho_{e'}} \chi_e(\rho_e, \rho_{e'})(V_{\rho_e} \otimes V_{(\rho_e')^*})$

- Standard lattice gauge theory : $\rho' = \rho^*$
- Simplicity constraints : $\rho' \neq \rho^*$, some representations are forbidden
- Factorizing models : ρ and ρ' decoupled

  - we can consider just one copy: anyon models (in condensed matter)

$\mathcal{H}_e = \oplus_{\rho_e} V_{\rho_e}$ ↓

Particles coupled to Chern Simons
Continuum limit : critical phase (massless excitations)
Hamiltonian topologically protected against perturbations

Spin Nets based on S_3

- Group of permutations of three elements
- Simplest group with intertwiner degrees of freedom (non-abelian)
- Formed by 6 elements: identity, three odd permutations (two-cycles), and two even permutations (three-cycles)
- Irreducible representations:

  - Trivial representation — $\rho = 1$ — $2 \otimes 2 = 1$
  - Sign representation — $\rho = 2$ — $2 \otimes 3 = 3$
  - Standard representation (two-dimensional) — $\rho = 3$ — $3 \otimes 3 = 1 \oplus 2 \oplus 3$

- Definition of our models: $C_v(\{\rho_e\}_{e \supset v}) = P(\{\rho_e\}_{e \supset v}) \left[\prod_{e \supset v} \tilde{E}_e(\rho_e) \right] P(\{\rho_e\}_{e \supset v})$

$$\tilde{E}(1)$$

$$\tilde{E}(2)$$

$$\tilde{E}(3) = \begin{pmatrix} \tilde{E}(3)_{11} & 0 \\ 0 & \tilde{E}(3)_{22} \end{pmatrix}$$

$$\longleftrightarrow \quad E(g) = E(hgh^{-1}) \quad \forall h \in \mathbb{Z}_2$$

Phase diagram

$$\tilde{E}(1) = 1 + \alpha + 2\beta + 2\gamma \qquad \tilde{E}(2) = 1 - \alpha - 2\beta + 2\gamma \qquad \tilde{E}(3) = \begin{pmatrix} 1+\alpha-\beta-\gamma & 0 \\ 0 & 1-\alpha+\beta-\gamma \end{pmatrix}$$

- **Lattice gauge theory models :** $\alpha = \beta \quad \longleftrightarrow \quad E(g) = E(g'gg'^{-1}) \quad \forall g' \in S_3$
  - **BF (S_3 order) :** $\alpha = \beta = \gamma = 0$ $\quad \lambda = 1$ **in** $(\rho_T, \rho'_T) = (1,1), (2,2), (3,3)$
  - **HT (disorder) :** $\alpha = \beta = \gamma = 1$ $\quad \lambda = 1$ **in** $(\rho_T, \rho'_T) = (1,1)$
  - **BF on $S_3/\mathbb{Z}_3$ ($\mathbb{Z}_2$ order) :** $\alpha = \beta = 0,\ \gamma = 1$ $\quad \lambda = 1$ **in** $(\rho_T, \rho'_T) = (1,1), (2,2)$

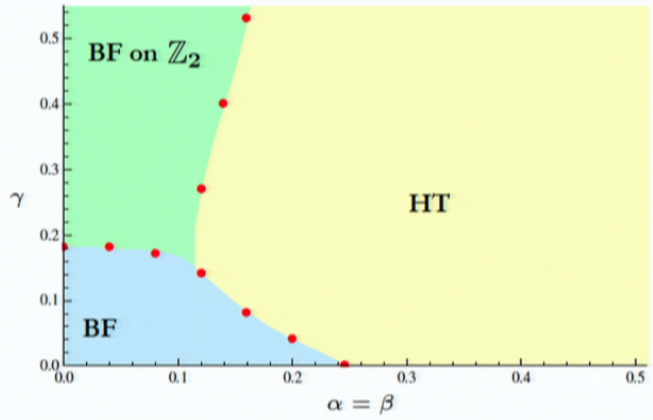

Phase diagram

$$\tilde{E}(1) = 1 + \alpha + 2\beta + 2\gamma \qquad \tilde{E}(2) = 1 - \alpha - 2\beta + 2\gamma \qquad \tilde{E}(3) = \begin{pmatrix} 1+\alpha-\beta-\gamma & 0 \\ 0 & 1-\alpha+\beta-\gamma \end{pmatrix}$$

- **Non-standard models :** $\alpha \neq \beta$
  - **Barret-Crane analog :** $\rho \neq 2\,,\ \alpha = 1,\ \beta = \gamma = 0 \quad \longleftrightarrow \quad E(g) = \int_{\mathbb{Z}_3} dh\delta(gh^{-1})$

It flows to BF, but very close to the phase transition

For low bond dimension it flows to a non-standard fixed point with $\rho \neq 2$!

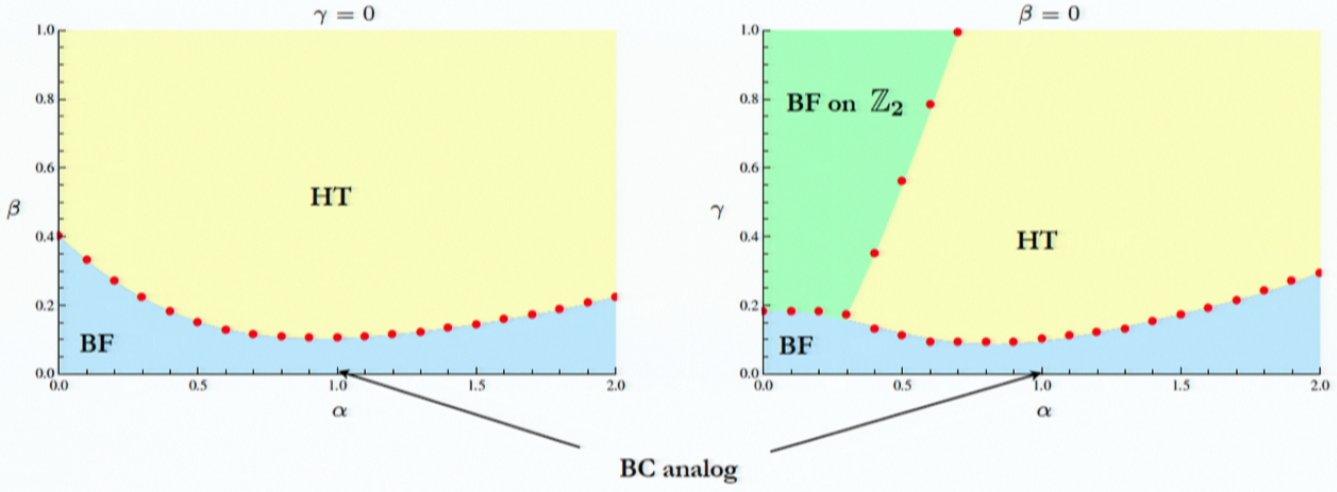

BF-HT phase transition

- Fine tuning to go away from dominating phases (BF or HT)

  - similar for BC spin foam model: need to fine tune face weights

[Khavkine & Christensen Class. Quant. Grav. 2007]

- Important to move away from standard LGT: linearizations around the fixed points of LGT only allow for $\rho' = \rho^*$

  - Migdal-Kadanoff-like approximations never consider $\rho' \neq \rho^*$

- Near a phase transition line the number of iterations to reach the fixed points increases

  - The model looks the same over a range of scales (iterations)
  - BC analog spin net is near this regime!

- The phase transition line might have more structure: additional fixed point

Non-standard fixed point

$\lambda = 1$ in $(\rho_T, \rho'_T) = (1,1), (1,3), (3,1), (3,3)$

$\rho \neq 2 \longrightarrow$ sign representation forbidden, simplicity constraint of BC analog

- Outside the range of original models: $\rho' \neq \rho^*$
- Factorizing form: $C_v(\{\rho_e\}, \{\rho'_e\}) = t(\{\rho_e\})t(\{\rho'_e\})$

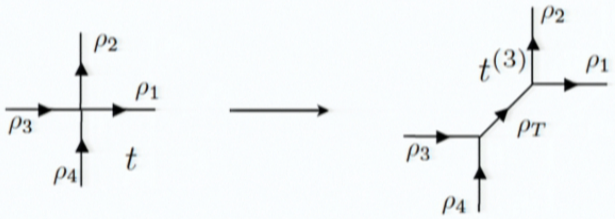

- $t^{(3)}$ defines a triangulation independent model : inv. under 2-2, 1-3, 3-1 Pachner moves

Outlook

- TRG keeping a single singular value per block
  - Most relevant d.o.f : reproduces phase diagram
  - Semi-analytical approximations for dynamics of intertwiners

- Other contraction schemes feasible for higher dimensions
  - e.g

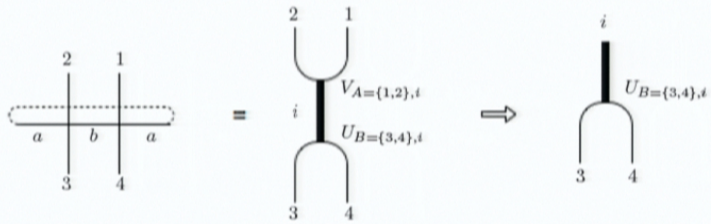

tested for the Ising model in 3D [S. Steinhaus, private communication]

- Corner transfer matrix renormalization [Baxter (1978), Nishino & Okunishi (1996), ...]

Outlook

- TRG keeping a single singular value per block
  - Most relevant d.o.f : reproduces phase diagram
  - Semi-analytical approximations for dynamics of intertwiners

- Other contraction schemes feasible for higher dimensions
  - e.g

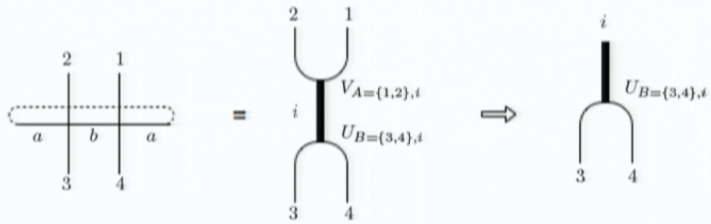

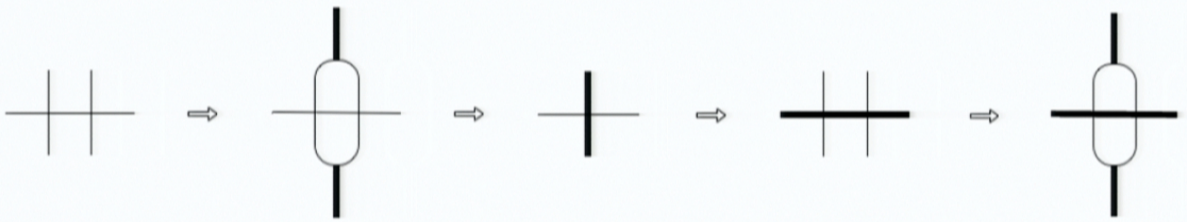

tested for the Ising model in 3D [S. Steinhaus, private communication]

- Corner transfer matrix renormalization [Baxter (1978), Nishino & Okunishi (1996), ...]

Outlook

- Enlarge space of models:

$\mathcal{H}_e = \oplus_{\rho_e}(V_{\rho_e} \otimes V_{\rho_e'^*}) \longrightarrow$ richer phase diagram

- Quantum groups $SU(2)_q$ with q root of unity [S. Steinhaus's talk]

  - study analogs of BC and EPRL

- Define observables and analyze their flow under renormalization

- Apply the lessons learnt with spin nets to spin foams!

Conclusions

- Non-abelian spin net models retain essential features of spin foam models: ⟶ simplicity constraints
- In vertex-model form we can analyze their renormalization flow under coarse-graining by using tensor network techniques
- Symmetry preserving algorithm : blocks labelled by intertwiner d.o.f.
- Approximation method to track these degrees of freedom: truncating SVD (the bigger the bond dimension the better the approximation)
- BC analog flows to BF but it is close to the phase transition
- Non-trivial fixed point detected, respecting BC simplicity constraints
- It defines a triangulation invariant model
- Need to fine tune to go away from lattice gauge theory fixed points
- The biggest singular values in each block seem to retain the most relevant physics

Renormalization of an SU(2) Tensorial Group Field Theory in 3d

Sylvain Carrozza

Albert Einstein Institute & Université Paris Sud

23/07/2013

Loops 13, Perimeter Institute.

Joint work with Daniele Oriti and Vincent Rivasseau.

Renormalization of an SU(2) Tensorial Group Field Theory in 3d

Sylvain Carrozza

Albert Einstein Institute & Université Paris Sud

23/07/2013

Loops 13, Perimeter Institute.

Joint work with Daniele Oriti and Vincent Rivasseau.

Introduction and motivations

Field theory interpretation of spin foam models: Group Field Theory (GFT).

- Main advantage: organizes the sum over foams.
- Main drawback: GFTs are poorly understood QFTs. In particular: renormalizability?

Challenge

Construct a renormalizable GFT for 4d quantum gravity.

Recent perspectives: significant help from tensor models $\rightarrow$ Tensorial Group Field Theories (TGFTs).

See plenary talks by Gurau and Rivasseau + parallel session on GFTs and tensor models.

Introduction and motivations

Field theory interpretation of spin foam models: Group Field Theory (GFT).

- Main advantage: organizes the sum over foams.
- Main drawback: GFTs are poorly understood QFTs. In particular: renormalizability?

Challenge

Construct a renormalizable GFT for 4d quantum gravity.

Recent perspectives: significant help from tensor models $\rightarrow$ Tensorial Group Field Theories (TGFTs).

See plenary talks by Gurau and Rivasseau + parallel session on GFTs and tensor models.

Introduction and motivations

Towards 4d spin foam QG models:

- First TGFTs, of a purely combinatorial nature:
  - $U(1)$ model in 4d: just-renormalizable up to φ^6 interactions, asymptotically free [Ben Geloun, Rivasseau '11, Ben Geloun '12]
  - $U(1)$ model in 3d: just-renormalizable up to φ^4 interactions, asymptotically free [Ben Geloun, Samary '12]
  - even more renormalizable models [Ben Geloun, Livine '12, Ben Geloun '13]
- Reintroducing the connection degrees of freedom:
  - $\mathrm{U}(1)$ toy-model in 4d [Oriti, Rivasseau, SC '12]: super-renormalizable;
  - $\mathrm{U}(1)$ toy-models in 5d and 6d: just-renormalizable [Samary, Vignes-Tourneret '12], asymptotically free [Samary '13];
  - $\mathrm{SU}(2)$ model in 3d: just-renormalizable [Oriti, Rivasseau, SC, '13].
- Simplicity constraints: future... [Riello '13]

Structure of a TGFT

- Dynamical variable: rank-d complex field

$$\varphi : (g_1, \dots, g_d) \ni G^d \mapsto \mathbb{C}\,,$$

with G a (compact) Lie group of dimension D.

- Partition function:

$$\mathcal{Z} = \int \mathrm{d}\mu_C(\varphi, \overline{\varphi})\, \mathrm{e}^{-S(\varphi,\overline{\varphi})}\,.$$

  - $S(\varphi, \overline{\varphi})$ is the interaction part of the action, and should be a sum of **local** terms.
  - Dynamics + geometrical constraints contained in the **Gaussian measure** $\mathrm{d}\mu_C$ with covariance C (i.e. 2nd moment):

$$\int \mathrm{d}\mu_C(\varphi, \overline{\varphi})\, \varphi(g_\ell)\overline{\varphi}(g'_\ell) = C(g_\ell; g'_\ell)$$

Structure of a TGFT

- Dynamical variable: rank-d complex field

$$\varphi : (g_1, \dots, g_d) \ni G^d \mapsto \mathbb{C}\,,$$

with G a (compact) Lie group of dimension D.

- Partition function:

$$\mathcal{Z} = \int \mathrm{d}\mu_C(\varphi, \overline{\varphi})\, \mathrm{e}^{-S(\varphi,\overline{\varphi})}\,.$$

  - $S(\varphi, \overline{\varphi})$ is the interaction part of the action, and should be a sum of **local** terms.
  - Dynamics + geometrical constraints contained in the **Gaussian measure** $\mathrm{d}\mu_C$ with covariance C (i.e. 2nd moment):

$$\int \mathrm{d}\mu_C(\varphi, \overline{\varphi})\, \varphi(g_\ell)\overline{\varphi}(g'_\ell) = C(g_\ell; g'_\ell)$$

Gaussian measure

We would like to construct TGFTs with:

- a built-in notion of scale i.e. a non-trivial propagator spectrum;
- a notion of discrete connection at the level of the amplitudes.

Particular realization that we consider:

- Gauge constraint:

$$\forall h \in G\,, \quad \varphi(hg_1, \dots, hg_d) = \varphi(g_1, \dots g_d)\,, \tag{1}$$

- supplemented by the non-trivial kernel (conservative choice, also justified by [Ben Geloun, Bonzom '11])

$$\left(m^2 - \sum_{\ell=1}^{d} \Delta_\ell\right)^{-1}. \tag{2}$$

This defines the measure $\mathrm{d}\mu_C$:

$$\int \mathrm{d}\mu_C(\varphi, \overline{\varphi})\, \varphi(g_\ell)\overline{\varphi}(g'_\ell) = C(g_\ell; g'_\ell) = \int_0^{+\infty} \mathrm{d}\alpha\, \mathrm{e}^{-\alpha m^2} \int \mathrm{d}h \prod_{\ell=1}^{d} K_\alpha(g_\ell h g'^{-1}_\ell)\,, \tag{3}$$

where K_α is the heat kernel on G at time α.

Gaussian measure

We would like to construct TGFTs with:

- a built-in notion of scale i.e. a non-trivial propagator spectrum;
- a notion of discrete connection at the level of the amplitudes.

Particular realization that we consider:

- Gauge constraint:

$$\forall h \in G\,, \quad \varphi(hg_1, \dots, hg_d) = \varphi(g_1, \dots g_d)\,, \tag{1}$$

- supplemented by the non-trivial kernel (conservative choice, also justified by [Ben Geloun, Bonzom '11])

$$\left(m^2 - \sum_{\ell=1}^{d} \Delta_\ell\right)^{-1}. \tag{2}$$

This defines the measure $\mathrm{d}\mu_C$:

$$\int \mathrm{d}\mu_C(\varphi, \overline{\varphi})\, \varphi(g_\ell)\overline{\varphi}(g'_\ell) = C(g_\ell; g'_\ell) = \int_0^{+\infty} \mathrm{d}\alpha\, \mathrm{e}^{-\alpha m^2} \int \mathrm{d}h \prod_{\ell=1}^{d} K_\alpha(g_\ell h g'^{-1}_\ell)\,, \tag{3}$$

where K_α is the heat kernel on G at time α.

Feynman graphs

- The amplitudes are indexed by $(d+1)$-colored graphs, obtained by connecting d-bubble vertices through propagators (dashed, color-0 lines).

  Example: 4-point graph with 3 vertices and 6 (internal) lines.

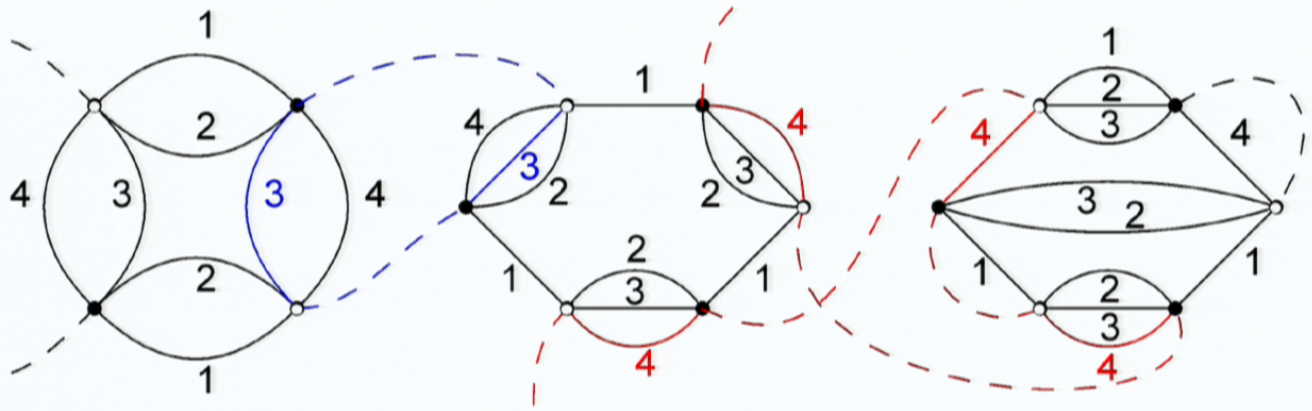

- Nomenclature:
  - $L(\mathcal{G})$ = set of (dotted) lines of a graph $\mathcal{G}$.
  - **Face of color ℓ** = connected set of (alternating) color-0 and color-ℓ lines.
  - $F(\mathcal{G})$ (resp. $F_{ext}(\mathcal{G})$) = set of internal (resp. external) i.e. closed (resp. open) faces of $\mathcal{G}$.

Amplitudes and gauge symmetry

- The amplitude of $\mathcal{G}$ depends on oriented products of group elements along its faces:

$$\begin{aligned}\mathcal{A}_{\mathcal{G}} &= \left[\prod_{e\in L(\mathcal{G})}\int \mathrm{d}\alpha_e\, e^{-m^2\alpha_e}\int \mathrm{d}h_e\right]\left(\prod_{f\in F(\mathcal{G})} K_{\alpha(f)}\left(\overrightarrow{\prod_{e\in\partial f}} h_e^{\epsilon_{ef}}\right)\right)\\ &\quad\left(\prod_{f\in F_{ext}(\mathcal{G})} K_{\alpha(f)}\left(g_{s(f)}\left[\overrightarrow{\prod_{e\in\partial f}} h_e^{\epsilon_{ef}}\right] g_{t(f)}^{-1}\right)\right),\\ &= \left[\prod_{e\in L(\mathcal{G})}\int \mathrm{d}\alpha_e\, e^{-m^2\alpha_e}\right]\{\textit{ Regularized Boulatov-like amplitudes }\}\end{aligned}$$

  where $\alpha(f)=\sum_{e\in\partial f}\alpha_e$, $g_{s(f)}$ and $g_{t(f)}$ are boundary variables, and $\epsilon_{ef}=\pm 1$ **when** $e\in\partial f$ **is the incidence matrix between oriented lines and faces.**

- A **gauge symmetry** associated to vertices ($h_e\mapsto g_{t(e)}h_e g_{s(e)}^{-1}$) allows to impose $h_e=\mathbf{1}$ along a maximal tree of (dotted) lines.

Amplitudes and gauge symmetry

- The amplitude of $\mathcal{G}$ depends on oriented products of group elements along its faces:

$$\begin{aligned}\mathcal{A}_{\mathcal{G}} &= \left[\prod_{e\in L(\mathcal{G})}\int \mathrm{d}\alpha_e\, e^{-m^2\alpha_e}\int \mathrm{d}h_e\right]\left(\prod_{f\in F(\mathcal{G})} K_{\alpha(f)}\left(\overrightarrow{\prod_{e\in\partial f}} h_e^{\epsilon_{ef}}\right)\right)\\ &\quad\left(\prod_{f\in F_{ext}(\mathcal{G})} K_{\alpha(f)}\left(g_{s(f)}\left[\overrightarrow{\prod_{e\in\partial f}} h_e^{\epsilon_{ef}}\right] g_{t(f)}^{-1}\right)\right),\\ &= \left[\prod_{e\in L(\mathcal{G})}\int \mathrm{d}\alpha_e\, e^{-m^2\alpha_e}\right]\{\ \textit{Regularized Boulatov-like amplitudes}\ \}\end{aligned}$$

  where $\alpha(f)=\sum_{e\in\partial f}\alpha_e$, $g_{s(f)}$ and $g_{t(f)}$ are boundary variables, and $\epsilon_{ef}=\pm 1$ **when $e\in\partial f$ is the incidence matrix between oriented lines and faces.**

- A **gauge symmetry** associated to vertices ($h_e\mapsto g_{t(e)}h_e g_{s(e)}^{-1}$) allows to impose $h_e=\mathbf{1}$ along a maximal tree of (dotted) lines.

Amplitudes and gauge symmetry

- The amplitude of $\mathcal{G}$ depends on oriented products of group elements along its faces:

$$\begin{aligned}\mathcal{A}_{\mathcal{G}} &= \left[\prod_{e\in L(\mathcal{G})}\int \mathrm{d}\alpha_e\, e^{-m^2\alpha_e}\int \mathrm{d}h_e\right]\left(\prod_{f\in F(\mathcal{G})} K_{\alpha(f)}\left(\overrightarrow{\prod_{e\in\partial f}} h_e^{\epsilon_{ef}}\right)\right)\\ &\quad\left(\prod_{f\in F_{ext}(\mathcal{G})} K_{\alpha(f)}\left(g_{s(f)}\left[\overrightarrow{\prod_{e\in\partial f}} h_e^{\epsilon_{ef}}\right] g_{t(f)}^{-1}\right)\right),\\ &= \left[\prod_{e\in L(\mathcal{G})}\int \mathrm{d}\alpha_e\, e^{-m^2\alpha_e}\right]\ \{\ \textit{Regularized Boulatov-like amplitudes}\ \}\end{aligned}$$

  where $\alpha(f)=\sum_{e\in\partial f}\alpha_e$, $g_{s(f)}$ and $g_{t(f)}$ are boundary variables, and $\epsilon_{ef}=\pm 1$ **when $e\in\partial f$ is the incidence matrix between oriented lines and faces.**

- A **gauge symmetry** associated to vertices ($h_e\mapsto g_{t(e)}h_e g_{s(e)}^{-1}$) allows to impose $h_e=\mathbf{1}$ along a maximal tree of (dotted) lines.

Classification of just-renormalizable models

Abelian power-counting theorem

The **degree of divergence** of a graph $\mathcal{H}$ is given by

$$\omega(\mathcal{H}) = -2L(\mathcal{H}) + D(F(\mathcal{H}) - R(\mathcal{H})) \tag{4}$$

$$\omega(\mathcal{H}) = D(d-2) - \frac{D(d-2)-2}{2}N \tag{5}$$

$$- \sum_{k=1}^{v_{max}/2} [D(d-2) - (D(d-2)-2)k]n_{2k} \tag{6}$$

$$+ 3\rho(\mathcal{H}) . \tag{7}$$

Type	d	D	v_{max}	ω
A	3	3	6	$3 - N/2 - 2n_2 - n_4 + 3\rho$
B	3	4	4	$4 - N - 2n_2 + 4\rho$
C	4	2	4	$4 - N - 2n_2 + 2\rho$
D	5	1	6	$3 - N/2 - 2n_2 - n_4 + \rho$
E	6	1	4	$4 - N - 2n_2 + \rho$

Table: Classification of potentially just-renormalizable models.

Classification of just-renormalizable models

Abelian power-counting theorem

The degree of divergence of a graph $\mathcal{H}$ is given by

$$\omega(\mathcal{H}) = -2L(\mathcal{H}) + D(F(\mathcal{H}) - R(\mathcal{H})) \tag{4}$$

$$\omega(\mathcal{H}) = D(d-2) - \frac{D(d-2)-2}{2}N \tag{5}$$

$$- \sum_{k=1}^{v_{max}/2} [D(d-2) - (D(d-2)-2)k]n_{2k} \tag{6}$$

$$+ 3\rho(\mathcal{H}) . \tag{7}$$

Type	d	D	v_{max}	ω
A	3	3	6	$3 - N/2 - 2n_2 - n_4 + 3\rho$
B	3	4	4	$4 - N - 2n_2 + 4\rho$
C	4	2	4	$4 - N - 2n_2 + 2\rho$
D	5	1	6	$3 - N/2 - 2n_2 - n_4 + \rho$
E	6	1	4	$4 - N - 2n_2 + \rho$

Table: Classification of potentially just-renormalizable models.

Classification of just-renormalizable models

Abelian power-counting theorem

The **degree of divergence** of a graph $\mathcal{H}$ is given by

$$\omega(\mathcal{H}) = -2L(\mathcal{H}) + D(F(\mathcal{H}) - R(\mathcal{H})) \tag{4}$$

$$\omega(\mathcal{H}) = D(d-2) - \frac{D(d-2)-2}{2}N \tag{5}$$

$$- \sum_{k=1}^{v_{max}/2} [D(d-2) - (D(d-2)-2)k]n_{2k} \tag{6}$$

$$+ 3\rho(\mathcal{H})\,. \tag{7}$$

Type	d	D	v_{max}	ω
A	3	3	6	$3 - N/2 - 2n_2 - n_4 + 3\rho$
B	3	4	4	$4 - N - 2n_2 + 4\rho$
C	4	2	4	$4 - N - 2n_2 + 2\rho$
D	5	1	6	$3 - N/2 - 2n_2 - n_4 + \rho$
E	6	1	4	$4 - N - 2n_2 + \rho$

Table: Classification of potentially just-renormalizable models.

The φ^6 just-renormalizable model: $G = \mathrm{SU}(2)$ and $d = 3$

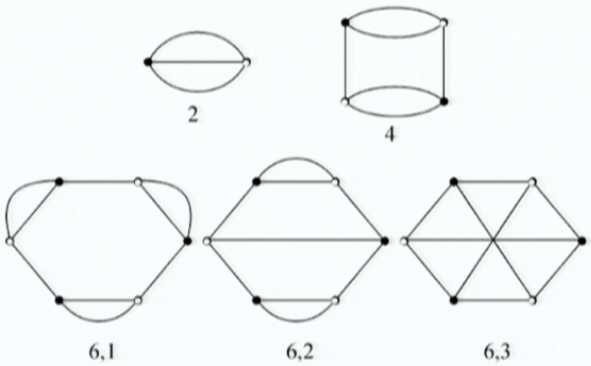

Figure: Possible bubble interactions.

$$\mathcal{Z}_\Lambda = \int \mathrm{d}\mu_{C^\Lambda}(\varphi, \overline{\varphi})\, \mathrm{e}^{-S_\Lambda(\varphi,\overline{\varphi})}\,. \tag{8}$$

$$S_\Lambda = t_4^\Lambda S_4 + t_{6,1}^\Lambda S_{6,1} + t_{6,2}^\Lambda S_{6,2} + CT_m^\Lambda S_m + CT_\varphi^\Lambda S_\varphi\,, \tag{9}$$

with:

$$S_m(\varphi,\overline{\varphi}) = \int [\mathrm{d}g]^3\, \varphi(g_1,g_2,g_3)\overline{\varphi}(g_1,g_2,g_3)\,, \tag{10}$$

$$S_\varphi(\varphi,\overline{\varphi}) = \int [\mathrm{d}g]^3\, \varphi(g_1,g_2,g_3)\left(-\sum_{l=1}^{3}\Delta_\ell\right)\overline{\varphi}(g_1,g_2,g_3)\,. \tag{11}$$

Divergent graphs

Degree of divergence:

$$\omega(\mathcal{H}) = 3 - \frac{N}{2} - 2n_2 - n_4 + 3\rho(\mathcal{H}/\mathcal{T}) \tag{12}$$

N	n_2	n_4	ρ	ω
6	0	0	0	0
4	0	0	0	1
4	0	1	0	0
2	0	0	0	2
2	0	1	0	1
2	0	2	0	0
2	1	0	0	0

Table: Classification of non-vacuum divergent graphs for $d = D = 3$.

2-point divergences $\Rightarrow$ mass and wave-function renormalization.

Coarse-graining high scale faces

Goal: reabsorb the divergences into the coupling constants, the mass, and the wave-function couter-terms.

Necessary condition: **divergent high subgraphs must be quasi-local, i.e. look like (connected) tensor invariants.**

Example: scales $i < j$

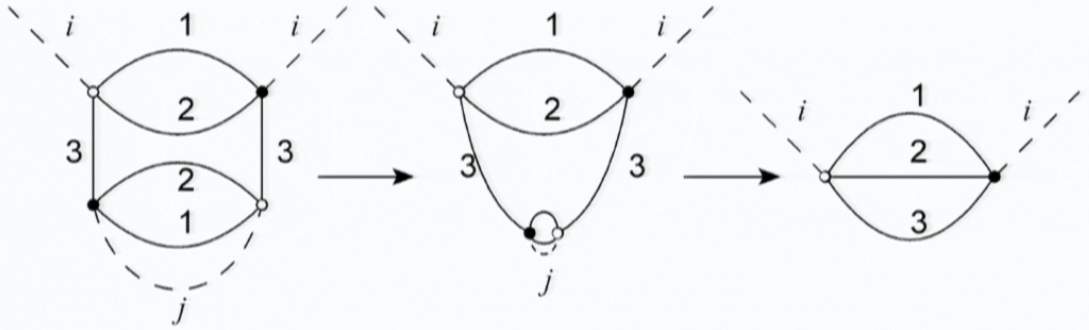

This is not automatic in TGFTs $\rightarrow$ **traciality**:

- flatness condition: the parallel transports must peak around $\mathbf{1}$ (up to gauge);
- combinatorial condition: connected boundary graph.

Results

- Perturbative renormalizability at all orders [Oriti , Rivasseau, SC '13]:
  - traciality of the divergent subgraphs (melonic);
  - multiscale expansion in a non-Abelian setting;
  - counter-terms indexed by face-connected subgraphs;
  - adaptation of the notion of Zimmermann forest to this context;
  - BPHZ theorem...
- Renormalization group flow [SC wip]:
  - effective field theory à la Wilson;
  - truncated flow equations;
  - asymptotic freedom?

Conclusions and outlook

We have now at our disposal:

- A general renormalization scheme for TGFTs with gauge invariance and non-Abelian groups;
- a TGFT renormalizable version of the Boulatov model.

Take away message

TGFTs seem mature enough to be applied to 4d quantum gravity models. Next step: simplicity constraints.

On the renormalization group flow of the cosmological constant in causal dynamical triangulations

Joshua H. Cooperman

Department of Physics
University of California, Davis

Loops 2013
Perimeter Institute for Theoretical Physics

23 July 2013

An introduction to causal dynamical triangulations

Quantum amplitude $\mathcal{A}[\Gamma] = \sum_{\substack{\mathcal{T}_c \\ \mathcal{T}_c|_{\partial\mathcal{T}_c}=\Gamma}} \mu(\mathcal{T}_c)\, e^{iS[\mathcal{T}_c]}$ Sum over all causal triangulations $\mathcal{T}_c$

An introduction to causal dynamical triangulations

Quantum amplitude $\mathcal{A}[\Gamma] = \sum_{\substack{\mathcal{T}_c \\ \mathcal{T}_c|_{\partial\mathcal{T}_c}=\Gamma}} \mu(\mathcal{T}_c)\, e^{iS[\mathcal{T}_c]}$ Sum over all causal triangulations $\mathcal{T}_c$

- Simplicial manifold possessing a global foliation by spacelike hypersurfaces all of the same topology

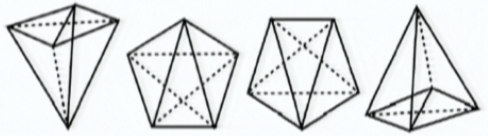

$l_{SL}^2 = a^2$ $l_{TL}^2 = -\alpha a^2$

An introduction to causal dynamical triangulations

Quantum amplitude $$\mathcal{A}[\Gamma] = \sum_{\substack{\mathcal{T}_c \\ \mathcal{T}_c|_{\partial\mathcal{T}_c}=\Gamma}} \mu(\mathcal{T}_c)\, e^{iS[\mathcal{T}_c]}$$ Sum over all causal triangulations $\mathcal{T}_c$

- Simplicial manifold possessing a global foliation by spacelike hypersurfaces all of the same topology

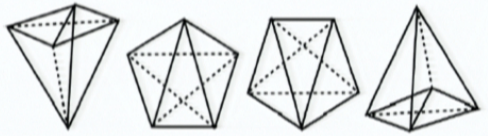

$l^2_{SL} = a^2$ $\quad$ $l^2_{TL} = -\alpha a^2$

Partition function $$\mathcal{Z}[\Gamma] = \sum_{\substack{\mathcal{T}_c \\ \mathcal{T}_c|_{\partial\mathcal{T}_c}=\Gamma}} \mu(\mathcal{T}_c)\, e^{-S^{(E)}[\mathcal{T}_c]}$$ Sum over all Wick rotated causal triangulations $\mathcal{T}_c$

An introduction to causal dynamical triangulations

Quantum amplitude $$\mathcal{A}[\Gamma] = \sum_{\substack{\mathcal{T}_c \\ \mathcal{T}_c|_{\partial\mathcal{T}_c}=\Gamma}} \mu(\mathcal{T}_c)\, e^{iS[\mathcal{T}_c]}$$ Sum over all causal triangulations $\mathcal{T}_c$

- Simplicial manifold possessing a global foliation by spacelike hypersurfaces all of the same topology

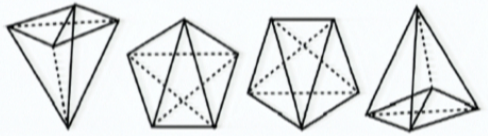

$l^2_{SL} = a^2$ $\quad$ $l^2_{TL} = -\alpha a^2$

Partition function $$\mathcal{Z}[\Gamma] = \sum_{\substack{\mathcal{T}_c \\ \mathcal{T}_c|_{\partial\mathcal{T}_c}=\Gamma}} \mu(\mathcal{T}_c)\, e^{-S^{(E)}[\mathcal{T}_c]}$$ Sum over all Wick rotated causal triangulations $\mathcal{T}_c$

- Run Monte Carlo simulations of representative causal triangulations at fixed T, N_4, and bare couplings

An introduction to causal dynamical triangulations

Quantum amplitude $$\mathcal{A}[\Gamma] = \sum_{\substack{\mathcal{T}_c \\ \mathcal{T}_c|_{\partial\mathcal{T}_c}=\Gamma}} \mu(\mathcal{T}_c)\, e^{iS[\mathcal{T}_c]}$$ Sum over all causal triangulations $\mathcal{T}_c$

- Simplicial manifold possessing a global foliation by spacelike hypersurfaces all of the same topology

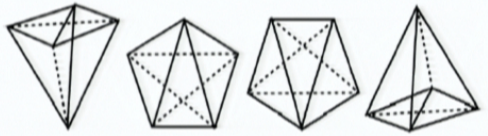

$l^2_{SL} = a^2$ $\quad$ $l^2_{TL} = -\alpha a^2$

Partition function $$\mathcal{Z}[\Gamma] = \sum_{\substack{\mathcal{T}_c \\ \mathcal{T}_c|_{\partial\mathcal{T}_c}=\Gamma}} \mu(\mathcal{T}_c)\, e^{-S^{(E)}[\mathcal{T}_c]}$$ Sum over all Wick rotated causal triangulations $\mathcal{T}_c$

- Run Monte Carlo simulations of representative causal triangulations at fixed T, N_4, and bare couplings

An introduction to causal dynamical triangulations

Quantum amplitude $$\mathcal{A}[\Gamma] = \sum_{\substack{\mathcal{T}_c \\ \mathcal{T}_c|_{\partial\mathcal{T}_c}=\Gamma}} \mu(\mathcal{T}_c)\, e^{iS[\mathcal{T}_c]}$$

Sum over all causal triangulations $\mathcal{T}_c$

- Simplicial manifold possessing a global foliation by spacelike hypersurfaces all of the same topology

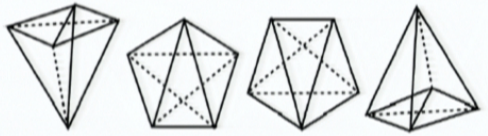

$$l^2_{SL} = a^2 \qquad l^2_{TL} = -\alpha a^2$$

Partition function $$\mathcal{Z}[\Gamma] = \sum_{\substack{\mathcal{T}_c \\ \mathcal{T}_c|_{\partial\mathcal{T}_c}=\Gamma}} \mu(\mathcal{T}_c)\, e^{-S^{(E)}[\mathcal{T}_c]}$$

Sum over all Wick rotated causal triangulations $\mathcal{T}_c$

- Run Monte Carlo simulations of representative causal triangulations at fixed T, N_4, and bare couplings
- Einstein gravity with positive cosmological constant for spacetime topology $\mathcal{S}^3 \times \mathcal{S}^1$

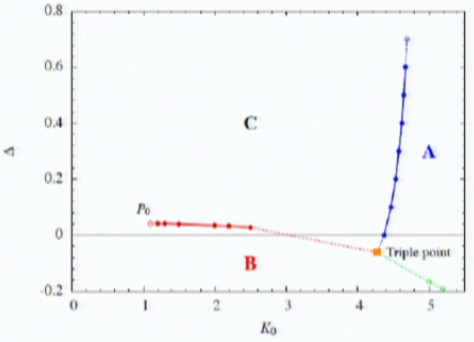

[Ambjørn *et al* 2012]

An effective description of phase C on large scales

Dynamical variable $N_3^{SL}(\tau)$

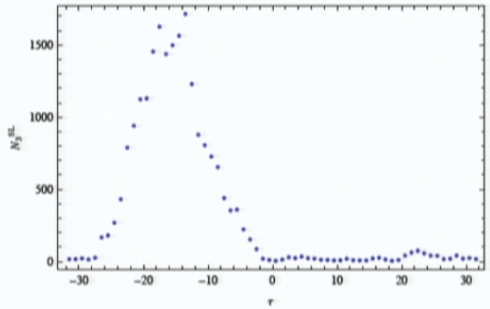

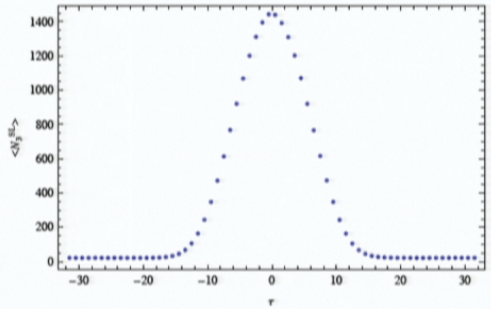

An effective description of phase C on large scales

Dynamical variable $N_3^{SL}(\tau)$

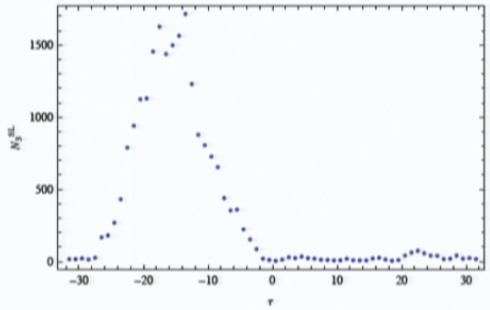

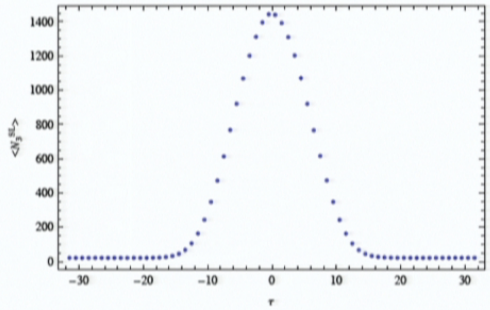

Deviation $n_3^{SL}(\tau) = N_3^{SL}(\tau) - \langle N_3^{SL}(\tau) \rangle$ from the ensemble average

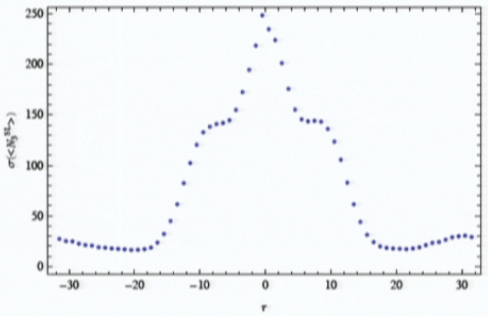

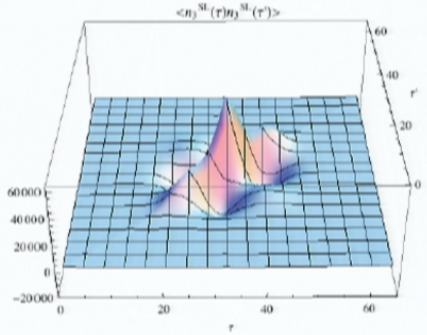

An effective description of phase C on large scales

Dynamical variable $N_3^{SL}(\tau)$

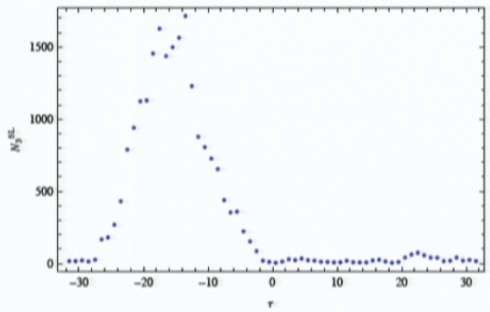

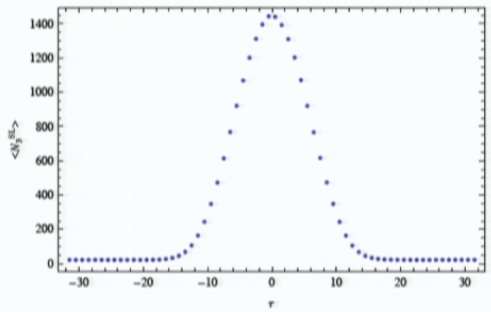

Deviation $n_3^{SL}(\tau) = N_3^{SL}(\tau) - \langle N_3^{SL}(\tau) \rangle$ from the ensemble average

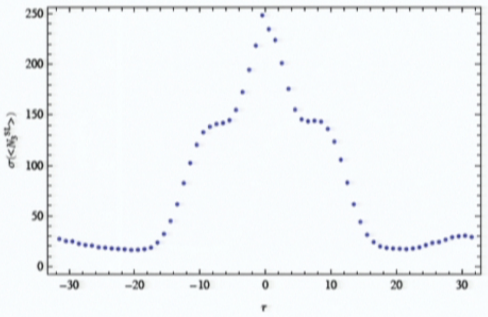

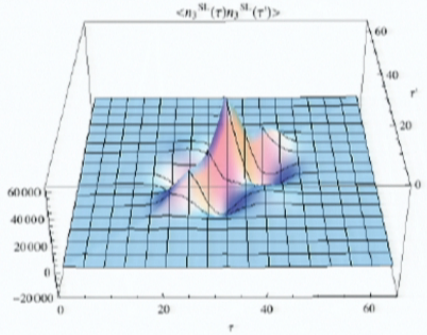

Numerically measured effective action for $N_3^{SL}(\tau)$ [Ambjørn *et al* 2005, 2008, 2012]

$$S_{\text{eff}}^{(E)}[N_3^{SL}(\tau)] = c_1 \sum_{\tau=1}^{T} \left\{ \frac{1}{N_3^{SL}(\tau)} \left[\frac{\Delta N_3^{SL}(\tau)}{\Delta \tau} \right]^2 + c_2 \left[N_3^{SL}(\tau) \right]^{1/3} - c_3 N_3^{SL}(\tau) \right\}$$

Aim and method

Aim

- Extract the renormalization group flow of the cosmological constant
  - Focus on the dimensionless product $G\Lambda$
  - Measure effective length scales in units of the Planck length l_P

Aim and method

Aim

- Extract the renormalization group flow of the cosmological constant
  - Focus on the dimensionless product $G\Lambda$
  - Measure effective length scales in units of the Planck length l_P

Method [Ambjørn *et al* 2008]

1. Fit the effective action $S^{(E)}_{\text{eff}}[N_3^{SL}(\tau)]$ to numerical measurements of $\langle N_3^{SL}(\tau)\rangle$ and $\langle n_3^{SL}(\tau) n_3^{SL}(\tau')\rangle$ to determine the effective couplings c_1, c_2, c_3, ...

Aim and method

Aim

- Extract the renormalization group flow of the cosmological constant
  - Focus on the dimensionless product $G\Lambda$
  - Measure effective length scales in units of the Planck length l_P

Method [Ambjørn *et al* 2008]

1. Fit the effective action $S^{(E)}_{\text{eff}}[N_3^{SL}(\tau)]$ to numerical measurements of $\langle N_3^{SL}(\tau)\rangle$ and $\langle n_3^{SL}(\tau) n_3^{SL}(\tau')\rangle$ to determine the effective couplings c_1, c_2, c_3, ...
2. Finite size scale the effective action $S^{(E)}_{\text{eff}}[N_3^{SL}(\tau)]$ towards the continuum limit to relate the effective couplings c_1, c_2, c_3, ... to the gravitational couplings G, Λ, ...
3. Analyze many different ensembles of causal triangulations to probe many different effective scales.

Aim and method

Aim

- Extract the renormalization group flow of the cosmological constant
  - Focus on the dimensionless product $G\Lambda$
  - Measure effective length scales in units of the Planck length l_P

Method [Ambjørn *et al* 2008]

1. Fit the effective action $S^{(E)}_{\text{eff}}[N_3^{SL}(\tau)]$ to numerical measurements of $\langle N_3^{SL}(\tau)\rangle$ and $\langle n_3^{SL}(\tau) n_3^{SL}(\tau')\rangle$ to determine the effective couplings c_1, c_2, c_3, ...
2. Finite size scale the effective action $S^{(E)}_{\text{eff}}[N_3^{SL}(\tau)]$ towards the continuum limit to relate the effective couplings c_1, c_2, c_3, ... to the gravitational couplings G, Λ, ...
3. Analyze many different ensembles of causal triangulations to probe many different effective scales.

Fit of the effective action $S_{\text{eff}}^{(E)}[N_3^{SL}(\tau)]$

Expand the effective action $S_{\text{eff}}^{(E)}[N_3^{SL}(\tau)]$ in powers of $n_3^{SL}(\tau)$ about $\langle N_3^{SL}(\tau)\rangle$

Fit of the effective action $S_{\text{eff}}^{(E)}[N_3^{SL}(\tau)]$

Expand the effective action $S_{\text{eff}}^{(E)}[N_3^{SL}(\tau)]$ in powers of $n_3^{SL}(\tau)$ about $\langle N_3^{SL}(\tau)\rangle$

0. Zeroth order in $n_3^{SL}(\tau)$
   - Fit discretization of $V_3(\eta)$ for Euclidean de Sitter spacetime to $\langle N_3^{SL}(\tau)\rangle$

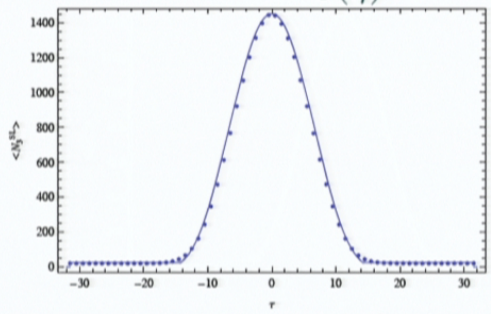

$$\langle N_3^{SL}(\tau)\rangle = \frac{\langle N_4^{(1,4)}\rangle c_3^{1/2}}{4}\cos^3\left(\frac{c_3^{1/2}\tau}{3}\right)$$

   - Determines c_2 in terms of c_3 and constrains c_3

Fit of the effective action $S^{(E)}_{\text{eff}}[N_3^{SL}(\tau)]$

Expand the effective action $S^{(E)}_{\text{eff}}[N_3^{SL}(\tau)]$ in powers of $n_3^{SL}(\tau)$ about $\langle N_3^{SL}(\tau)\rangle$

0. Zeroth order in $n_3^{SL}(\tau)$
   - Fit discretization of $V_3(\eta)$ for Euclidean de Sitter spacetime to $\langle N_3^{SL}(\tau)\rangle$

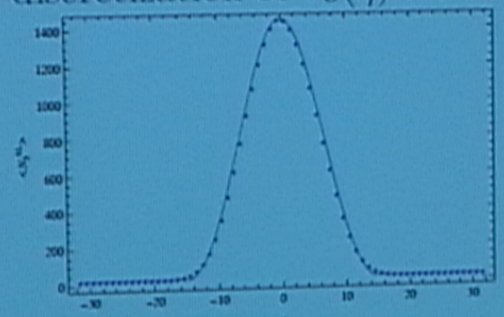

$$\langle N_3^{SL}(\tau)\rangle = \frac{\langle N_4^{(1,4)}\rangle c_3^{1/2}}{4}\cos^3\left(\frac{c_3^{1/2}\tau}{3}\right)$$

   - Determines c_2 in terms of c_3 and constrains c_3

1. First order in $n_3^{SL}(\tau)$
   - Expect $0 \approx \left.\frac{\delta S_{\text{eff}}[N_3^{SL}(\tau)]}{\delta n_3^{SL}(\tau')}\right|_{n_3^{SL}(\tau')=0}$ since $\langle N_3^{SL}(\tau)\rangle$ is an extremum
   - Constrains c_1 and c_3

Fit of the effective action $S_{\text{eff}}^{(E)}[N_3^{SL}(\tau)]$

Expand the effective action $S_{\text{eff}}^{(E)}[N_3^{SL}(\tau)]$ in powers of $n_3^{SL}(\tau)$ about $\langle N_3^{SL}(\tau)\rangle$

0. Zeroth order in $n_3^{SL}(\tau)$
   - Fit discretization of $V_3(\eta)$ for Euclidean de Sitter spacetime to $\langle N_3^{SL}(\tau)\rangle$

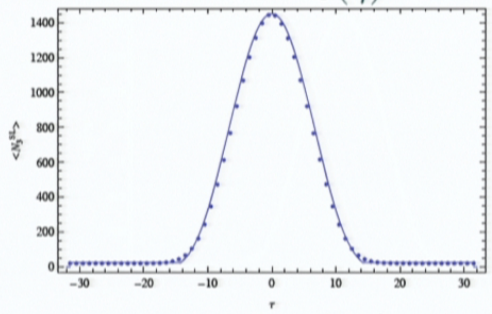

$$\langle N_3^{SL}(\tau)\rangle = \frac{\langle N_4^{(1,4)}\rangle c_3^{1/2}}{4}\cos^3\left(\frac{c_3^{1/2}\tau}{3}\right)$$

   - Determines c_2 in terms of c_3 and constrains c_3

1. First order in $n_3^{SL}(\tau)$
   - Expect $0 \approx \left.\frac{\delta S_{\text{eff}}[N_3^{SL}(\tau)]}{\delta n_3^{SL}(\tau')}\right|_{n_3^{SL}(\tau')=0}$ since $\langle N_3^{SL}(\tau)\rangle$ is an extremum
   - Constrains c_1 and c_3

Fit of the effective action $S^{(E)}_{\text{eff}}[N_3^{SL}(\tau)]$

Expand the effective action $S^{(E)}_{\text{eff}}[N_3^{SL}(\tau)]$ in powers of $n_3^{SL}(\tau)$ about $\langle N_3^{SL}(\tau)\rangle$

0. Zeroth order in $n_3^{SL}(\tau)$
   - Fit discretization of $V_3(\eta)$ for Euclidean de Sitter spacetime to $\langle N_3^{SL}(\tau)\rangle$

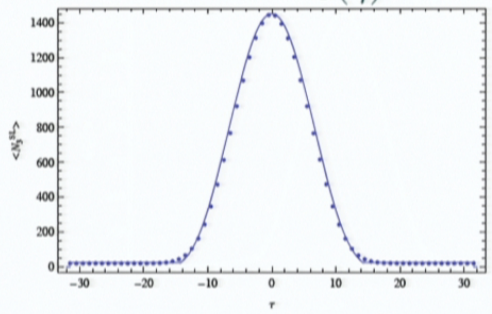

$$\langle N_3^{SL}(\tau)\rangle = \frac{\langle N_4^{(1,4)}\rangle c_3^{1/2}}{4}\cos^3\left(\frac{c_3^{1/2}\tau}{3}\right)$$

   - Determines c_2 in terms of c_3 and constrains c_3

1. First order in $n_3^{SL}(\tau)$
   - Expect $0 \approx \left.\frac{\delta S_{\text{eff}}[N_3^{SL}(\tau)]}{\delta n_3^{SL}(\tau')}\right|_{n_3^{SL}(\tau')=0}$ since $\langle N_3^{SL}(\tau)\rangle$ is an extremum
   - Constrains c_1 and c_3

2. Second order in $n_3^{SL}(\tau)$
   - Expect $\langle n_3^{SL}(\tau')n_3^{SL}(\tau'')\rangle^{-1} = \frac{1}{\hbar}\left.\frac{\delta^2 S_{\text{eff}}[N_3^{SL}(\tau)]}{\delta n_3^{SL}(\tau')\delta n_3^{SL}(\tau'')}\right|_{\substack{n_3^{SL}(\tau')=0\\ n_3^{SL}(\tau'')=0}}$
   - Constrains c_1 and c_3

Fit of the effective action $S^{(E)}_{\text{eff}}[N_3^{SL}(\tau)]$

Expand the effective action $S^{(E)}_{\text{eff}}[N_3^{SL}(\tau)]$ in powers of $n_3^{SL}(\tau)$ about $\langle N_3^{SL}(\tau)\rangle$

0. Zeroth order in $n_3^{SL}(\tau)$
   - Fit discretization of $V_3(\eta)$ for Euclidean de Sitter spacetime to $\langle N_3^{SL}(\tau)\rangle$

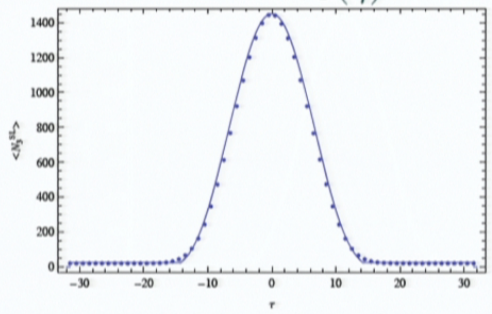

$$\langle N_3^{SL}(\tau)\rangle = \frac{\langle N_4^{(1,4)}\rangle c_3^{1/2}}{4}\cos^3\left(\frac{c_3^{1/2}\tau}{3}\right)$$

   - Determines c_2 in terms of c_3 and constrains c_3
1. First order in $n_3^{SL}(\tau)$
   - Expect $0 \approx \left.\frac{\delta S_{\text{eff}}[N_3^{SL}(\tau)]}{\delta n_3^{SL}(\tau')}\right|_{n_3^{SL}(\tau')=0}$ since $\langle N_3^{SL}(\tau)\rangle$ is an extremum
   - Constrains c_1 and c_3
2. Second order in $n_3^{SL}(\tau)$
   - Expect $\langle n_3^{SL}(\tau')n_3^{SL}(\tau'')\rangle^{-1} = \frac{1}{\hbar}\left.\frac{\delta^2 S_{\text{eff}}[N_3^{SL}(\tau)]}{\delta n_3^{SL}(\tau')\delta n_3^{SL}(\tau'')}\right|_{\substack{n_3^{SL}(\tau')=0\\ n_3^{SL}(\tau'')=0}}$
   - Constrains c_1 and c_3

Finite size scaling of the effective action $S_{\rm eff}^{(E)}[N_3^{SL}(\tau)]$

Scale τ and $N_3^{SL}(\tau)$ to find continuum limit of the effective action $S_{\rm eff}^{(E)}[N_3^{SL}(\tau)]$

Finite size scaling of the effective action $S^{(E)}_{\rm eff}[N_3^{SL}(\tau)]$

Scale τ and $N_3^{SL}(\tau)$ to find continuum limit of the effective action $S^{(E)}_{\rm eff}[N_3^{SL}(\tau)]$

- Naive continuum limit $\quad V_4 = \lim_{\substack{N_4\to\infty \\ a\to 0}} C_4 N_4 a^4$
  - Expect $\tau \longrightarrow \tilde{\tau} = \frac{\tau}{N_4^{1/4}}$ to scale into $\tilde{\eta} = \frac{\eta}{V_4^{1/4}}$
  - Expect $N_3^{SL}(\tau) \longrightarrow \tilde{N}_3^{SL}(\tilde{\tau}) = \frac{N_3^{SL}(\tau)}{N_4^{3/4}}$ to scale into $\tilde{V}_3(\tilde{\eta}) = \frac{V_3(\eta)}{V_4^{3/4}}$

Finite size scaling of the effective action $S^{(E)}_{\rm eff}[N_3^{SL}(\tau)]$

Scale τ and $N_3^{SL}(\tau)$ to find continuum limit of the effective action $S^{(E)}_{\rm eff}[N_3^{SL}(\tau)]$

- Naive continuum limit $\quad V_4 = \lim_{\substack{N_4\to\infty \\ a\to 0}} C_4 N_4 a^4$
  - Expect $\tau \longrightarrow \tilde{\tau} = \frac{\tau}{N_4^{1/4}}$ to scale into $\tilde{\eta} = \frac{\eta}{V_4^{1/4}}$
  - Expect $N_3^{SL}(\tau) \longrightarrow \tilde{N}_3^{SL}(\tilde{\tau}) = \frac{N_3^{SL}(\tau)}{N_4^{3/4}}$ to scale into $\tilde{V}_3(\tilde{\eta}) = \frac{V_3(\eta)}{V_4^{3/4}}$
- Evidence for the naive continuum limit

Scaled correlator $\langle \tilde{N}_3^{SL}(\tilde{\tau}) \tilde{N}_3^{SL}(\tilde{\tau}') \rangle$

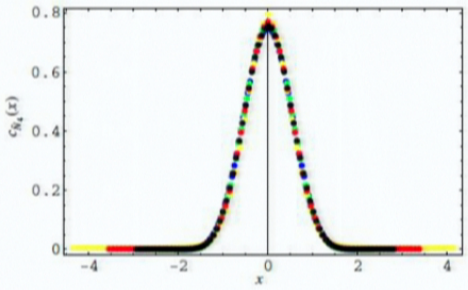

[Ambjørn *et al* 2005]

Scaled spectral dimension $D_s(\tilde{\sigma})$

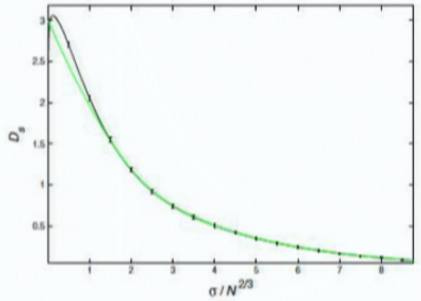

[Benedetti and Henson 2009]

Finite size scaling of the effective action $S^{(E)}_{\rm eff}[N_3^{SL}(\tau)]$

Scale τ and $N_3^{SL}(\tau)$ to find continuum limit of the effective action $S^{(E)}_{\rm eff}[N_3^{SL}(\tau)]$

- Naive continuum limit $\quad V_4 = \lim_{\substack{N_4\to\infty \\ a\to 0}} C_4 N_4 a^4$
  - Expect $\tau \longrightarrow \tilde{\tau} = \frac{\tau}{N_4^{1/4}}$ to scale into $\tilde{\eta} = \frac{\eta}{V_4^{1/4}}$
  - Expect $N_3^{SL}(\tau) \longrightarrow \tilde{N}_3^{SL}(\tilde{\tau}) = \frac{N_3^{SL}(\tau)}{N_4^{3/4}}$ to scale into $\tilde{V}_3(\tilde{\eta}) = \frac{V_3(\eta)}{V_4^{3/4}}$
- Evidence for the naive continuum limit

Scaled correlator $\langle \tilde{N}_3^{SL}(\tilde{\tau}) \tilde{N}_3^{SL}(\tilde{\tau}') \rangle$

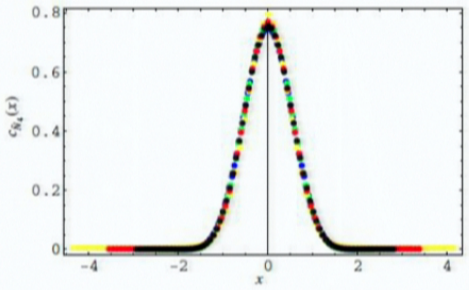

[Ambjørn *et al* 2005]

Scaled spectral dimension $D_s(\tilde{\sigma})$

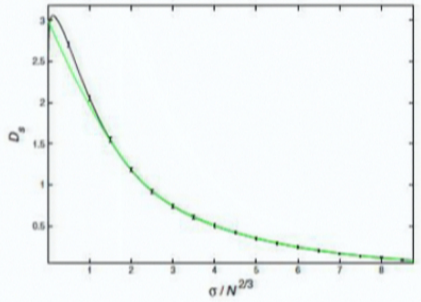

[Benedetti and Henson 2009]

Finite size scaling of the effective action $S^{(E)}_{\rm eff}[N_3^{SL}(\tau)]$

Scale τ and $N_3^{SL}(\tau)$ to find continuum limit of the effective action $S^{(E)}_{\rm eff}[N_3^{SL}(\tau)]$

- Naive continuum limit $\quad V_4 = \lim_{\substack{N_4\to\infty \\ a\to 0}} C_4 N_4 a^4$
  - Expect $\tau \longrightarrow \tilde{\tau} = \frac{\tau}{N_4^{1/4}}$ to scale into $\tilde{\eta} = \frac{\eta}{V_4^{1/4}}$
  - Expect $N_3^{SL}(\tau) \longrightarrow \tilde{N}_3^{SL}(\tilde{\tau}) = \frac{N_3^{SL}(\tau)}{N_4^{3/4}}$ to scale into $\tilde{V}_3(\tilde{\eta}) = \frac{V_3(\eta)}{V_4^{3/4}}$
- Evidence for the naive continuum limit

Scaled correlator $\langle \tilde{N}_3^{SL}(\tilde{\tau})\tilde{N}_3^{SL}(\tilde{\tau}')\rangle$

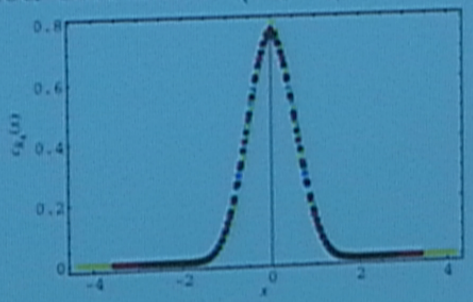

[Ambjørn *et al* 2005]

Scaled spectral dimension $D_s(\tilde{\sigma})$

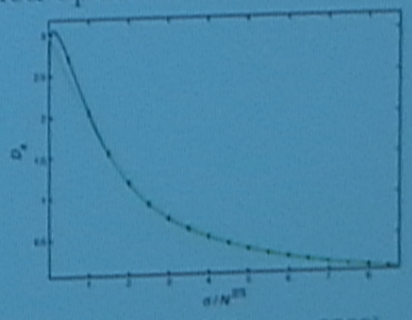

[Benedetti and Henson 2009]

- Continuum limit of the effective action $S^{(E)}_{\rm eff}[N_3^{SL}(\tau)]$

$$S^{(E)}_{EH}[V_3(\eta)] = \frac{1}{24\pi G}\int \mathrm{d}\eta \sqrt{g_{\eta\eta}} \left\{ \frac{g^{\eta\eta}}{V_3(\eta)} \left[\frac{\mathrm{d}V_3(\eta)}{\mathrm{d}\eta}\right]^2 + 9(2\pi^2)^{2/3} V_3^{1/3}(\eta) - 3\Lambda V_3(\eta) \right\}$$

Renormalization group flow of $G\Lambda$

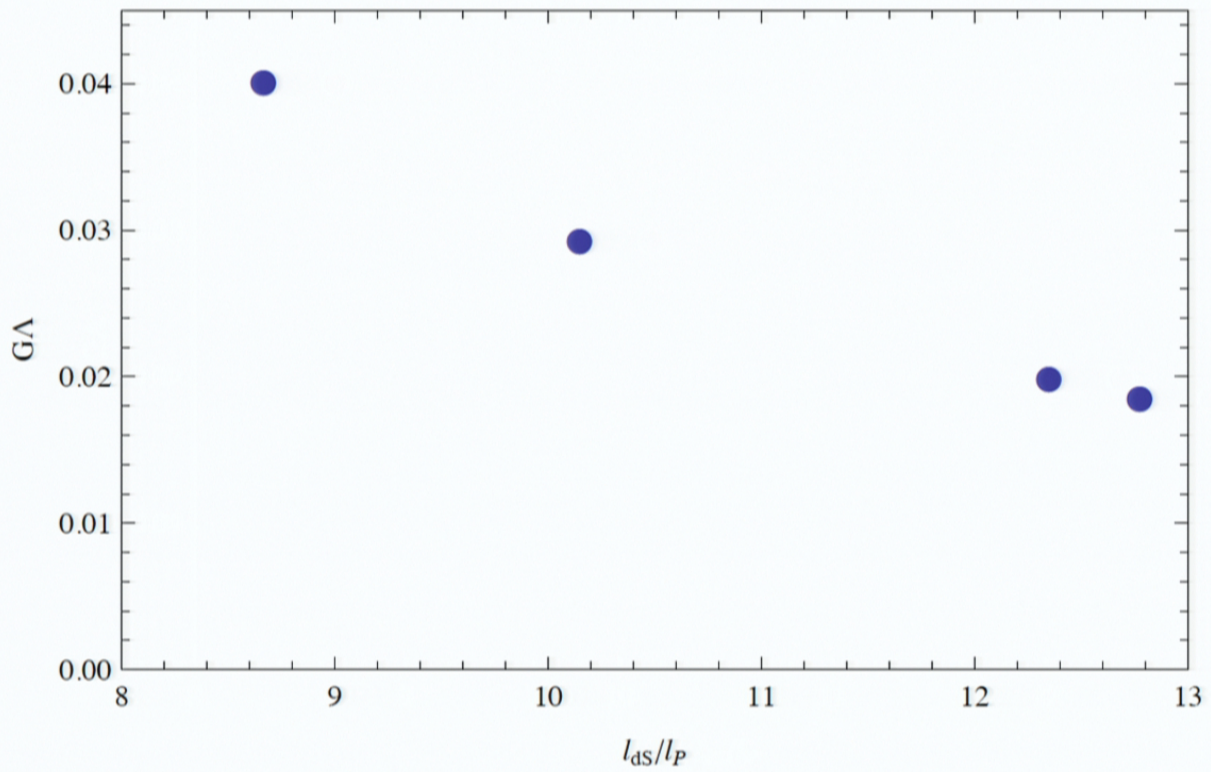

Continuing research

- Probe more of the renormalization group flow by generating more ensembles of causal triangulations
- Consistency checks of the method
  - Validity of the expansion of the effective action
  - Inclusion of higher order terms in the effective action
- Determine regimes of validity of the Einstein-Hilbert truncation

Acknowledgments

- Steve Carlip for considerable advice and guidance
- Rajesh Kommu for writing the Davis group's code
- Christian Anderson for improving and extending the Davis group's code
- Jonah Miller for improving and extending the Davis group's code
- Adam Getchell for managing numerical simulations